



A Journal of the Gesellschaft Deutscher Chemiker

# Angewandte Chemie

GDCh

International Edition

www.angewandte.org

## Accepted Article

**Title:** Role of Torsional Dynamics on Hole and Exciton Stabilization in pi-Stacked Assemblies: Design of Novel Rigid Torsionomers of a Cofacial Bifluorene

**Authors:** Denan Wang, Maxim Ivanov, Damian Kokkin, John Loman, Jin-zhe Cai, Rajendra Rathore, and Scott Reid

This manuscript has been accepted after peer review and appears as an Accepted Article online prior to editing, proofing, and formal publication of the final Version of Record (VoR). This work is currently citable by using the Digital Object Identifier (DOI) given below. The VoR will be published online in Early View as soon as possible and may be different to this Accepted Article as a result of editing. Readers should obtain the VoR from the journal website shown below when it is published to ensure accuracy of information. The authors are responsible for the content of this Accepted Article.

**To be cited as:** *Angew. Chem. Int. Ed.* 10.1002/anie.201804337  
*Angew. Chem.* 10.1002/ange.201804337

**Link to VoR:** <http://dx.doi.org/10.1002/anie.201804337>  
<http://dx.doi.org/10.1002/ange.201804337>

# Role of Torsional Dynamics on Hole and Exciton Stabilization in $\pi$ -Stacked Assemblies: Design of Novel Rigid Torsionomers of a Cofacial Bifluorene

Denan Wang, Maxim V. Ivanov, Damian Kokkin, John Loman, Jin-Zhe Cai, Scott A. Reid\* and Rajendra Rathore†

In memory of Rajendra Rathore

**Abstract:** Efficient exciton and charge delocalization across  $\pi$ -stacked assemblies is of critical importance in biological systems and functional polymeric materials. To examine the requirements for exciton and hole stabilization, we report the design, synthesis, and characterization of a novel set of cofacial bifluorene (**F2**) torsionomers: unhindered (model) <sup>Me</sup>**F2**, sterically hindered <sup>tBu</sup>**F2**, and cyclophane-like <sup>C</sup>**F2**, where fluorenes are rigidly locked in a perfect sandwich orientation via two methylene linkers. This set of carefully designed bichromophores with varied torsional rigidity and orbital overlap shows that exciton stabilization requires a perfect sandwich-like arrangement, as evidenced by strong excimeric-like emission only in <sup>C</sup>**F2** and <sup>Me</sup>**F2**. In contrast, hole delocalization is less geometrically restrictive and occurs even in sterically hindered <sup>tBu</sup>**F2**, as judged by 160 mV hole stabilization and a near-IR band in the spectrum of its cation radical. These findings underscore the diverse requirements for charge and energy delocalization across  $\pi$ -stacked assemblies.

Charge and energy dynamics across  $\pi$ -stacked assemblies is of critical importance in biological systems as well in the performance of functional materials.<sup>1-3</sup> Various  $\pi$ -stacked dimers capable of excimer formation and charge-resonance stabilization based upon benzene,<sup>4-8</sup> fluorene,<sup>9-12</sup> pyrene<sup>13,14</sup> and other aromatic donors<sup>15-18</sup> have served as model systems to gain fundamental insight into key factors controlling charge/energy stabilization. These studies have established that the extent of the cationic charge (i.e., hole) and exciton stabilization/delocalization is dependent on the orbital overlap between the chromophores, and is optimal when the  $\pi$ -stacked assembly adopts a perfect sandwich-like arrangement, where orbital overlap and electronic coupling are at their maxima.<sup>10,11</sup>

Building upon this work, recent studies comparing a model covalently linked fluorene dimer **F2** with the van der Waals dimer of fluorene, (**F**)<sub>2</sub>, have shown that the geometrical requirements for hole and exciton stabilization are distinct.<sup>10,11</sup> In particular, while their ionization potentials (IPs) are identical, excimeric emission at the sandwich-like geometries is shifted to longer wavelength in **F2** as compared to (**F**)<sub>2</sub>. Thus, a slight displacement from the ideal overlap leads to a less stabilized excimer in (**F**)<sub>2</sub>, while cation radical stabilization remains unchanged. In the same context, in covalently linked

polyfluorenes (**F***n*, *n* = 2-7) the cationic charge is delocalized over multiple fluorenes,<sup>19,20</sup> while exciton delocalization is limited to two fluorenes.<sup>21</sup>

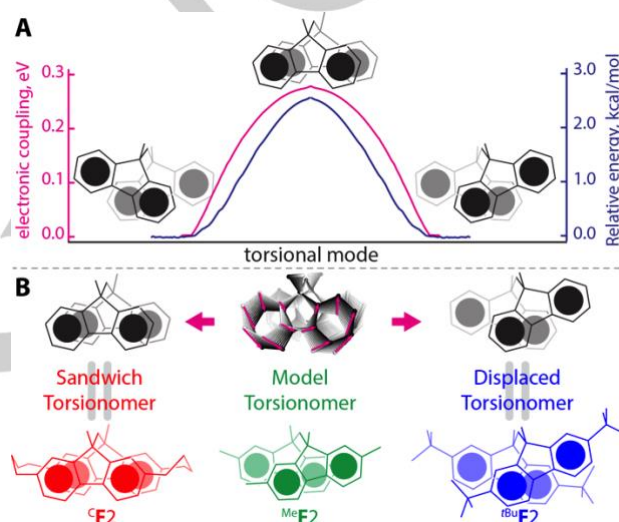


**Figure 1.** A. The electronic coupling and relative energy of **F2** calculated using B1LYP40-D3/6-31G(d)+PCM(CH<sub>2</sub>Cl<sub>2</sub>) along the intrinsic reaction coordinate connecting two displaced conformations. The structure with the maximal coupling and energy is a transition state with the imaginary frequency ( $i12.1$  cm<sup>-1</sup>) corresponding to the torsional motion. B. Schematic representation of the torsional mode in **F2**. Incorporation of a methylene linker (i.e., <sup>C</sup>**F2**) and substituents (i.e., <sup>Me</sup>**F2** and <sup>tBu</sup>**F2**) produces various torsionomers of **F2**.

Importantly, the dynamics of hole and exciton transfer in **F***n* is modulated by a low-frequency torsional mode between adjacent units, as evidenced in the broad and largely unresolved band in the gas-phase excitation spectrum of **F2**.<sup>10</sup> Indeed, calculations show that the activation barrier for interconversion between two mirror images displaced conformers of **F2** is only 3 kcal/mol, yet the electronic coupling along the interconversion coordinate varies between 0.0-0.3 eV (Figure 1A).

In order to probe the effect of cofaciality on the hole and exciton stabilization in  $\pi$ -stacked systems, we synthesized three rigid torsionomers of **F2**, i.e., cofacial bifluorenes that differ by the extent of their cofaciality along the torsional coordinate via methylene linkers or substituents (Figure 1B). In a cyclophane-like bifluorene <sup>C</sup>**F2**, a pair of four-methylene linkers ensures that the relative arrangement of fluorenes is nearly identical to that found in the excimer and dimer cation radical of unsubstituted **F2**. In contrast, bulky <sup>tBu</sup> groups in <sup>tBu</sup>**F2** guarantee that the sandwich-like arrangement is highly energetically unfavorable due to increased steric hindrance. We then compare the redox

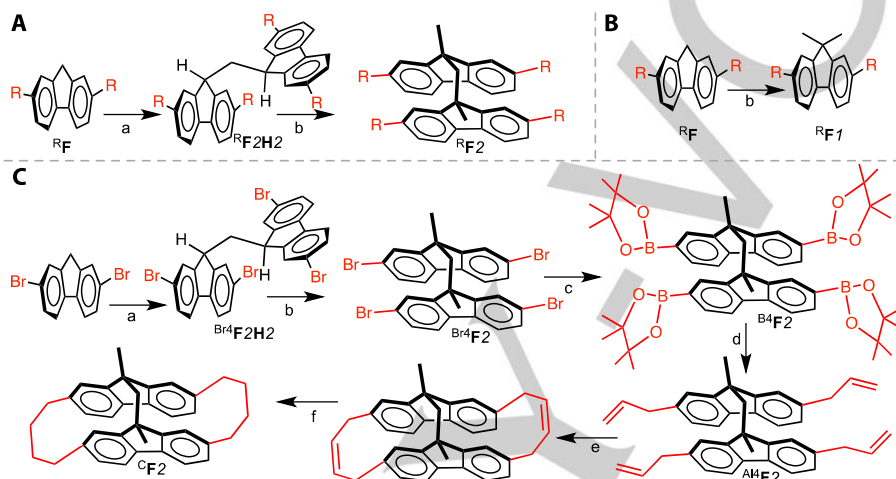
[\*] Dr. D. Wang, Dr. M. V. Ivanov, Dr. D. Kokkin, John Loman, Jin-Zhe Cai, Prof. S. A. Reid and Prof. Rajendra Rathore  
Department of Chemistry, Marquette University  
Milwaukee, WI 53201-1881 (USA)  
E-mail: scott.reid@marquette.edu

† Deceased February 16, 2018

and optoelectronic properties of the two torsionomers with those of model monomeric  $^{\text{Me}}\text{F1}/^{\text{tBu}}\text{F1}$  and model bichromophoric  $^{\text{Me}}\text{F2}$  whose geometrical properties are nearly identical to those of unsubstituted  $\text{F2}$ .

The bifluorene  $^{\text{R}}\text{F2H2}$  precursor was generated by the condensation reaction between readily available<sup>22,23</sup>  $^{\text{R}}\text{F}$  and 0.5 equivalent of paraformaldehyde with potassium *tert*-butyl oxide catalyst (Scheme 1A). Desired bi- and mono-fluorenes (i.e.,  $^{\text{R}}\text{F2}$  and  $^{\text{R}}\text{F1}$ ) are readily produced through the methylation of  $^{\text{R}}\text{F2H2}/^{\text{R}}\text{F}$  with MeI and potassium *tert*-butyl oxide as base (Scheme 1A/B). Synthesis of  $^{\text{C}}\text{F2}$  was carried out by following the procedure shown in Scheme 1C. First, the intermediate  $^{\text{Br4}}\text{F2}$

was generated by condensation of 2,7-dibromofluorene into  $^{\text{Br4}}\text{F2H2}$  followed by its methylation. The bromide was then converted to a boron ester using Pd(dppf)Cl<sub>2</sub> catalyst, which was reacted with allyl bromide to produce  $^{\text{Al4}}\text{F2}$ . Intramolecular olefin metathesis reaction allowed us to prepare the  $^{\text{C}}\text{F2}$  precursor in good yield, which was then subjected to Pd/C catalyzed hydrogenation, producing  $^{\text{C}}\text{F2}$  as a final product. The  $^{\text{R}}\text{F2}$  and  $^{\text{C}}\text{F2}$  torsionomers and their model compounds  $^{\text{R}}\text{F1}$  were fully characterized by <sup>1</sup>H/<sup>13</sup>C NMR spectroscopy (Figure 2A) and X-ray crystallography (Figure 2B); see Supporting Information for full details.



**Scheme 1.** a. 10 % mol KO<sup>t</sup>Bu, paraformaldehyde 0.5 eq, DMF, 20 °C 2 hour; b. KO<sup>t</sup>Bu 3 eq, MeI 3 eq, THF, 0 °C 12 h; c. (BPin)<sub>2</sub> 4.1 eq, KOAc 4.2 eq, Pd(dppf)Cl<sub>2</sub> 5% mol, 1,4-dioxane, reflux 12 hours; d. Allyl bromide 8 eq, Na<sub>2</sub>CO<sub>3</sub> 10 eq, Pd(PPh<sub>3</sub>)<sub>4</sub>, 1,2-dimethoxyethane, reflux 12 hours; e. Grubbs's II 2 % mol, benzene, rt 24 hours; f. H<sub>2</sub>, Pd/C, benzene, 2 hours.

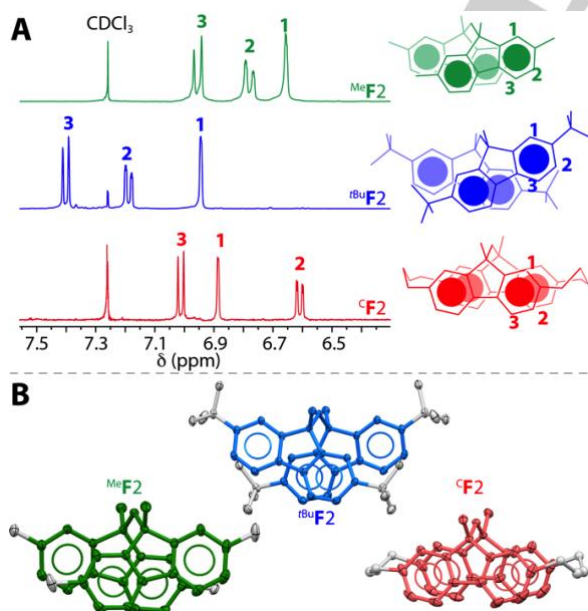


**Figure 2.** A. Partial <sup>1</sup>H NMR spectra of  $^{\text{Me}}\text{F2}$ ,  $^{\text{tBu}}\text{F2}$  and  $^{\text{C}}\text{F2}$  in CDCl<sub>3</sub> at 22 °C. B. ORTEP diagrams (50% diagram) of  $^{\text{Me}}\text{F2}$ ,  $^{\text{tBu}}\text{F2}$  and  $^{\text{C}}\text{F2}$  highlighting varied cofaciality of the torsionomers.

The characteristic absorption bands in the electronic spectra of  $^{\text{C}}\text{F2}$ ,  $^{\text{Me}}\text{F2}$  and  $^{\text{tBu}}\text{F2}$  are comprised of similar vibronic features and the wavelength of the absorption maximum is nearly invariant, i.e.,  $\lambda_{\text{max}} = 272 \pm 2$  nm (Figure 3). In contrast, emission spectra of  $\text{F2}$  derivatives display a strong dependence on the cofaciality between fluorene moieties (Figure 2). First, emission spectrum of  $^{\text{C}}\text{F2}$  shows a broad excimeric-like band at 402 nm with the lifetime ( $\tau$ ) of 3.8 ns. While the emission spectrum of  $^{\text{Me}}\text{F2}$  displays a similar excimeric band at 400 nm ( $\tau = 6.5$  ns), it also contains a weak band at 325 nm ( $\tau = 2.4$  ns), which corresponds to the region where emission of  $^{\text{Me}}\text{F1}$  monomer occurs (Figure S3 in the Supporting Information). This indicates that two minima must be present on the potential energy surface (PES) of the S<sub>1</sub> excited state of  $^{\text{Me}}\text{F2}$ . Indeed, TD-DFT calculations at the benchmarked<sup>12,24,25</sup> B1LYP40-D3/6-31G(d)+PCM(CH<sub>2</sub>Cl<sub>2</sub>) revealed the presence of two equilibrium structures of  $^{\text{Me}}\text{F2}$  on the excited state PES, with different exciton delocalization as represented by the transition-density plots in Figure 3. In the global-minimum excimeric sandwich-like structure, the exciton is delocalized over both fluorenes, while in the higher-energy displaced  $^{\text{Me}}\text{F2}$ , the exciton is localized on a single fluorene.

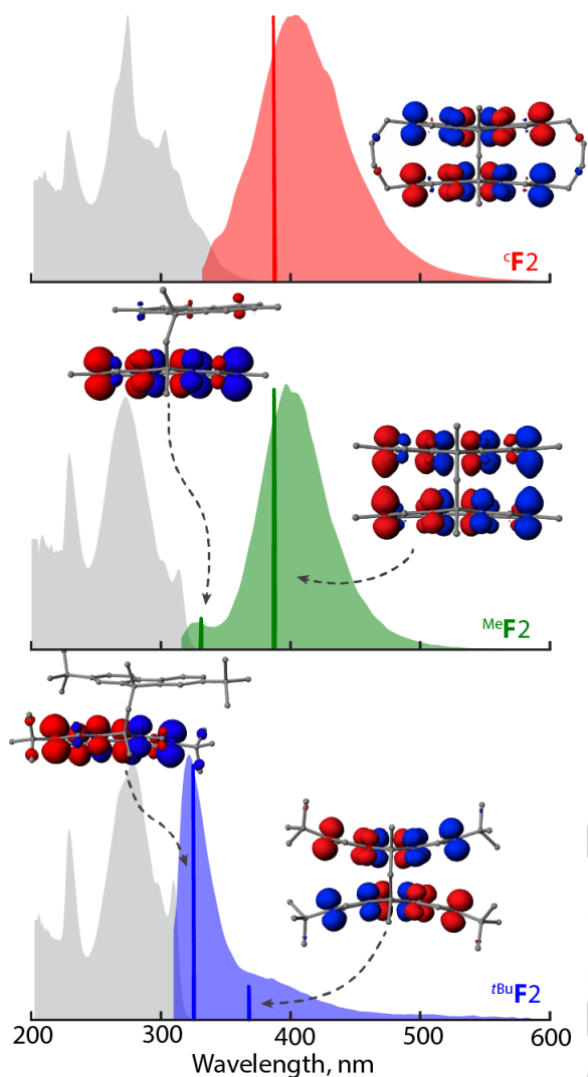


**Figure 3.** Absorption (grey) and emission (colored) spectra of  ${}^{\text{C}}\text{F}2$ ,  ${}^{\text{Me}}\text{F}2$  and  ${}^{\text{tBu}}\text{F}2$  in  $\text{CH}_2\text{Cl}_2$  at 22 °C. Sticks represent the emission wavelength calculated using TD-B1LYP40-D3/6-31G(d)+PCM( $\text{CH}_2\text{Cl}_2$ ). Transition-density plots are shown for the equilibrium structures of  ${}^{\text{C}}\text{F}2$ ,  ${}^{\text{Me}}\text{F}2$  and  ${}^{\text{tBu}}\text{F}2$ .

In contrast to unhindered  ${}^{\text{Me}}\text{F}2$ , the emission spectrum of sterically hindered  ${}^{\text{tBu}}\text{F}2$  displays strong monomeric and weak excimeric bands at 325 and 380 nm, with corresponding lifetimes of 0.4 ns and 1.5 ns, respectively. This suggests that the steric hindrance imposed by the bulky *t*Bu groups must destabilize a sandwich-like conformation in favor of the conformation where two fluorenes are displaced. Indeed, TD-DFT calculations showed the presence of two energetically similar equilibrium structures on the excited state PES of  ${}^{\text{tBu}}\text{F}2$ , corresponding to a sandwich-like conformation with exciton delocalized over both fluorenes and a displaced conformation with exciton fully localized on a single fluorene (Figure 3).

Cyclic voltammograms of  ${}^{\text{C}}\text{F}2$ ,  ${}^{\text{Me}}\text{F}2$  and  ${}^{\text{tBu}}\text{F}2$  show (Figure 4A) two reversible oxidation waves, with the first oxidation potential ( $E_{\text{ox}}$ ) increasing *gradually* from 0.66 to 0.77 to 0.86 V vs  $\text{Fc}/\text{Fc}^+$ , respectively. Comparison with the appropriate model compounds ( ${}^{\text{Me}}\text{F}1$  and  ${}^{\text{tBu}}\text{F}1$ ) shows that stabilization of the

cationic charge, i.e.,  $\Delta E_{\text{ox}} = E_{\text{ox}}({}^{\text{R}}\text{F}1) - E_{\text{ox}}({}^{\text{R}}\text{F}2)$ , is largest for  ${}^{\text{C}}\text{F}2$  ( $\Delta E_{\text{ox}} = 360$  mV) and decreases as the concomitant energetic penalty of adopting a sandwich-like arrangement increases in  ${}^{\text{Me}}\text{F}2$  ( $\Delta E_{\text{ox}} = 250$  mV) and  ${}^{\text{tBu}}\text{F}2$  ( $\Delta E_{\text{ox}} = 160$  mV). Despite the significant steric hindrance imposed by *t*Bu groups in  ${}^{\text{tBu}}\text{F}2$ , the hole stabilization of 160 mV remains significant, highlighting our prior finding that a hole can be stabilized even when there is a minimal orbital overlap.<sup>10,11</sup>

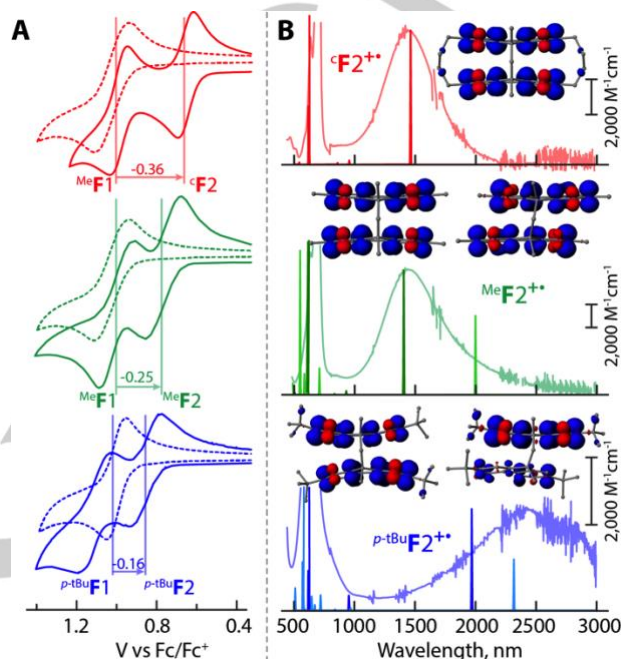


**Figure 4.** A. Cyclic voltammograms of 2 mM  ${}^{\text{C}}\text{F}2$ ,  ${}^{\text{Me}}\text{F}2$ ,  ${}^{\text{tBu}}\text{F}2$  (solid lines) and their corresponding monomeric model compounds (dashed lines) in  $\text{CH}_2\text{Cl}_2$  (0.1 M *n*-Bu<sub>4</sub>NPF<sub>6</sub>) at a scan rate of 100 mVs<sup>-1</sup> and 22 °C. B. Electronic absorption spectra of  ${}^{\text{C}}\text{F}2^{+}$ ,  ${}^{\text{Me}}\text{F}2^{+}$  and  ${}^{\text{tBu}}\text{F}2^{+}$  in  $\text{CH}_2\text{Cl}_2$  at 22 °C. Sticks represent excitation wavelength calculated using TD-B1LYP40-D3/6-31G(d)+PCM( $\text{CH}_2\text{Cl}_2$ ); dark colour corresponds to the sandwich-like structure and light colour corresponds to the displaced structure of  ${}^{\text{R}}\text{F}2$ .

We generated the cation radicals of  ${}^{\text{Me}}\text{F}2$ ,  ${}^{\text{tBu}}\text{F}2$ , and  ${}^{\text{C}}\text{F}2$  via quantitative<sup>26</sup> redox titrations using robust aromatic oxidants [THEO<sup>+</sup>][SbCl<sub>6</sub><sup>-</sup>] and NAP<sup>+</sup>SbCl<sub>6</sub> (see details in the Supporting Information).<sup>27</sup> Reproducible spectra of both  ${}^{\text{C}}\text{F}2^{+}$  and  ${}^{\text{Me}}\text{F}2^{+}$  show a nearly identical intense intervalence band centered at 1418 nm (Figure 4B), signifying that the  ${}^{\text{Me}}\text{F}2^{+}$  structure is identical to that of  ${}^{\text{C}}\text{F}2^{+}$ , i.e. corresponding to a sandwich-like arrangement of fluorenes, and the cationic charge is delocalized over both fluorenes via strong through-space electronic coupling. Indeed, (TD)-DFT calculations confirmed that the intense near-IR band corresponds to sandwich-like conformations of  ${}^{\text{C}}\text{F}2^{+}$  and  ${}^{\text{Me}}\text{F}2^{+}$ , where the charge/spin is delocalized over both fluorenes (Figure 4B). Our calculations also predict a displaced conformation of  ${}^{\text{Me}}\text{F}2^{+}$  that lies 1.4 kcal/mol higher in energy than the sandwich-like structure, and also displays spin/charge delocalization over both fluorenes, suggesting that even a minimal through-space orbital overlap is sufficient to promote hole delocalization in bifluorenes. This lies in contrast to the

excited state of  ${}^{\text{Me}}\text{F2}^+$ , where in the displaced conformation the exciton is localized on a single fluorene (Figure 3).

The electronic spectrum of  ${}^{\text{tBu}}\text{F2}^{2+}$  shows a much less intense intervalence band that is shifted to longer wavelength (2400 nm), suggesting a reduced electronic coupling and/or increased reorganization energy in  ${}^{\text{tBu}}\text{F2}^{2+}$  as compared to those in  ${}^{\text{C}}\text{F2}^{2+}$  and  ${}^{\text{Me}}\text{F2}^{2+}$ . DFT calculations showed that two energetically similar ( $\Delta G = 3.5$  kcal/mol) conformations of  ${}^{\text{tBu}}\text{F2}^{2+}$  may exist. The sandwich-like arrangement displays a significant puckering of the fluorene moieties due to the steric hindrance from bulky  ${}^{\text{tBu}}$  groups, yet the spin/charge remains delocalized over both fluorenes. In the displaced  ${}^{\text{tBu}}\text{F2}^{2+}$ , the spin/charge is largely localized on a single fluorene, due to the significant displacement and therefore reduced orbital overlap/electronic coupling.

Additional insights come from gas-phase spectra of the three torsionomers, obtained via laser induced fluorescence (LIF) spectroscopy using a heated supersonic nozzle; details are provided in the Supporting Information. As shown in Figure 5, the differences in these spectra are striking. The spectrum of  ${}^{\text{Me}}\text{F2}$  is similar to that of  $\text{F2}$  in displaying a broad and largely unresolved profile (Figure 5A); the breadth is explained in the terms of an underlying progression in the torsional motion which is broadened by the fast dynamics and strong modulation of the electronic coupling (Figure 1A). The underlying progression is clearly seen in the spectrum of  ${}^{\text{tBu}}\text{F2}$  (Figure 5B), absent any spectral broadening. On the other hand, the spectrum of  ${}^{\text{C}}\text{F2}$  (Figure 5C) is both sharp and distinct, and strikingly red-shifted. Here, the torsional libration is quenched and the Franck-Condon active vibration corresponds to a "breathing" type motion of the two subunits (see Figure S14 in Supporting Information). The dramatic consequences of steric hindrance in the  ${}^{\text{tBu}}\text{F2}$  derivative can be further seen in a comparison with unsubstituted  $\text{F2}$  (Figure 5D). Here, the underlying torsional progression is clearly evidenced, as the breadth of the spectra is similar. A more detailed analysis of these spectra is beyond the scope of this article and will be reported in future.

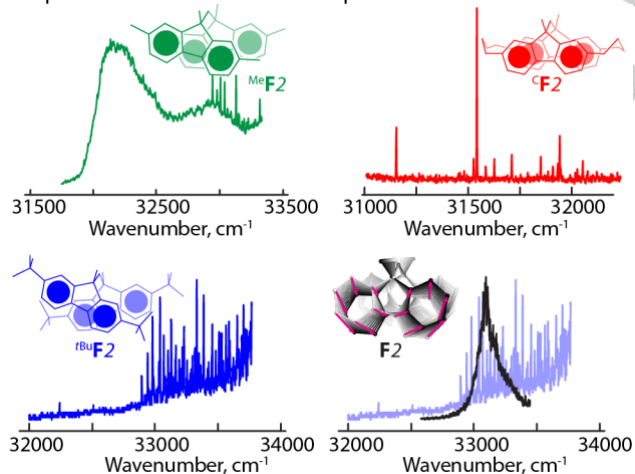


**Figure 5.** Laser induced fluorescence spectra of  ${}^{\text{Me}}\text{F2}$  (green),  ${}^{\text{tBu}}\text{F2}$  (blue),  ${}^{\text{C}}\text{F2}$  (red) and  $\text{F2}$  (black) in the gas-phase. Sharp transitions in the spectrum of  ${}^{\text{Me}}\text{F2}$  reflect monomeric impurity. Comparison of the LIF spectra of  $\text{F2}$  (black) with  ${}^{\text{tBu}}\text{F2}$  (blue) shows the underlying torsional progression.

In this study, we have used a set of novel torsionomers to examine the contrasting requirements for exciton and hole stabilization in  $\pi$ -stacked assemblies. Exciton stabilization requires a perfect sandwich-like arrangement, as evidenced by the presence of strong excimeric-like emission only in  ${}^{\text{C}}\text{F2}$  and  ${}^{\text{Me}}\text{F2}$ . In contrast, cationic charge can be delocalized even for structures where the path to cofaciality is sterically hindered, i.e.  ${}^{\text{tBu}}\text{F2}$ , as judged by the 160 mV hole stabilization and the presence of a near-IR transition in its cation radical spectrum. These findings underscore important design principles for next generation optoelectronic materials.

## Acknowledgements

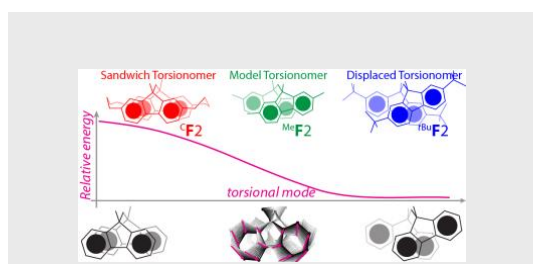
We thank the NSF (CHE-1508677) and NIH (R01-HL112639-04) for financial support. The calculations were performed on the high-performance computing cluster Père at Marquette University and XSEDE.

**Keywords:**  $\pi$ -stacking • charge delocalization • exciton delocalization

- [1] G. I. Livshits, A. Stern, D. Rotem, N. Borovok, G. Eidelshstein, A. Migliore, E. Penzo, S. J. Wind, R. Di Felice, S. S. Skourtis, *Nat. Nanotechnol.* **2014**, *9*, 1040.
- [2] Z. Zheng, N. R. Tummala, Y. -T. Fu, V. Coropceanu, J. -L. Brédas, *ACS Appl. Mater. Interfaces.* **2017**, *9*, 18095-18102.
- [3] C. Kaufmann, W. Kim, A. Nowak-Król, Y. Hong, D. Kim, F. Würthner, *J. Am. Chem. Soc.* **2018**, *140*, 4253-4258.
- [4] P. Ottiger, H. Köppel, S. Leutwyler, *Chem. Sci.* **2015**, *6*, 6059-6068.
- [5] M. Miyazaki, M. Fujii, *Phys. Chem. Chem. Phys.* **2015**, *17*, 25989-25997.
- [6] R. Kusaka, Y. Inokuchi, T. Ebata, *J. Chem. Phys.* **2012**, *136*, 044304.
- [7] P. A. Pieniazek, S. E. Bradforth, A. I. Krylov, *J. Chem. Phys.* **2008**, *129*, 074104.
- [8] E. S. S. Iyer, A. Sadybekov, O. Lioubashevski, A. I. Krylov, S. Ruhman, *J. Phys. Chem. A.* **2017**, *121*, 1962-1975.
- [9] J. Vura-Weis, S. H. Abdelwahed, R. Shukla, R. Rathore, M. A. Ratner, M. R. Wasielewski, *Science.* **2010**, *328*, 1547-1550.
- [10] N. Reilly, M. Ivanov, B. Uhler, M. Talipov, R. Rathore, S. A. Reid, *J. Phys. Chem. Lett.* **2016**, *7*, 3042-3045.
- [11] B. Uhler, M. V. Ivanov, D. Kokkin, N. Reilly, R. Rathore, S. A. Reid, *J. Phys. Chem. C.* **2017**, *121*, 15580-15588.
- [12] D. Kokkin, M. V. Ivanov, J. Loman, J. -Z. Cai, R. Rathore, S. A. Reid, *J. Phys. Chem. Lett.* **2018**, *9*, 2058-2061.
- [13] K. Kawai, T. Kimura, H. Yoshida, A. Sugimoto, S. Tojo, M. Fujitsuka, T. Majima, *Bull. Chem. Soc. Jpn.* **2006**, *79*, 312-316.
- [14] S. Samori, M. Fujitsuka, T. Majima, *Res. Chem. Intermed.* **2013**, *39*, 449-461.
- [15] Y. Gao, H. Liu, S. Zhang, Y. Shen, Y. Ge, B. Yang, *Phys. Chem. Chem. Phys.* **2018**, *20*, 12129-12137.
- [16] O. P. Dimitriev, Y. P. Piryatinski, Y. L. Slominskii, *J. Phys. Chem. Lett.* **2018**, *9*, 2138-2143.
- [17] B. L. Cannon, D. L. Kellis, L. K. Patten, P. H. Davis, J. Lee, E. Graugnard, B. Yurke, W. B. Knowlton, *J. Phys. Chem. A.* **2017**, *121*, 6905-6916.
- [18] J. K. Kochi, R. Rathore, P. L. Magueres, *J. Org. Chem.* **2000**, *65*, 6826-6836.
- [19] M. V. Ivanov, N. J. Reilly, B. Uhler, D. Kokkin, R. Rathore, S. A. Reid, *J. Phys. Chem. Lett.* **2017**, *8*, 5272-5276.
- [20] R. Rathore, S. H. Abdelwahed, I. A. Guzei, *J. Am. Chem. Soc.* **2003**, *125*, 8712-8713.

- [21] M. R. Talipov, M. V. Ivanov, S. A. Reid, R. Rathore, *J. Phys. Chem. Lett.* **2016**, *7*, 2915-2920.
- [22] M. W. Haenel, H. Irgartinger, C. Krieger, *Chem. Ber.*, *118*, 144-162.
- [23] J. Wang, W. Wan, H. Jiang, Y. Gao, X. Jiang, H. Lin, W. Zhao, J. Hao, *Org. Lett.* **2010**, *12*, 3874-3877.
- [24] M. R. Talipov, A. Boddada, Q. K. Timerghazin, R. Rathore, *J. Phys. Chem. C* **2014**, *118*, 21400-21408.
- [25] M. Ivanov, M. Talipov, T. Navale, R. Rathore, *J. Phys. Chem. C* **2018**, *122*, 2539-2545.
- [26] M. R. Talipov, A. Boddada, M. M. Hossain, R. Rathore, *J. Phys. Org. Chem.* **2015**, *29*, 227-233.
- [27] Talipov, M. R.; Rathore, R. Robust Aromatic Cation Radicals as Redox Tunable Oxidants. In *Organic Redox Systems: Synthesis, Properties, and Applications*; ; John Wiley & Sons: Hoboken, NJ, 2015; pp 131.

## COMMUNICATION



**Design and synthesis of the torsionomers of cofacial bifuorene:** A novel set of carefully designed pi-stacked bichromophores with varied rigidity and orbital overlap demonstrates disparate requirements for the exciton and cationic charge delocalization in pi-stacked assemblies.

Denan Wang, Maxim V. Ivanov, Damian Kokkin, John Loman, Jin-Zhe Cai, Scott A. Reid\* and Rajendra Rathore<sup>†</sup>

Page No. – Page No.

**Role of Torsional Dynamics on Hole and Exciton Stabilization in  $\pi$ -Stacked Assemblies: Design and Synthesis of Rigid Torsionomers of a Model Cofacial Bifuorene**

Accepted Manuscript